Introduction to GPDs

Matthias Burkardt

New Mexico State University

September 27, 2016

Outline

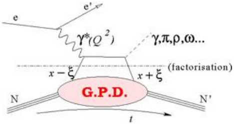

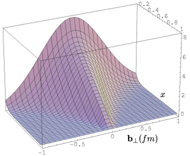

- GPDs $\xrightarrow{FT} q(x, \mathbf{b}_\perp)$ '3d imaging'
- $\perp$ polarization $\Rightarrow \perp$ deformation
- $\mathcal{L}^q_{JM} - L^q_{Ji}$ = change in OAM as quark leaves nucleon (due to torque from FSI)
- Summary

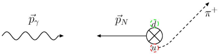

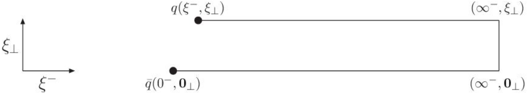

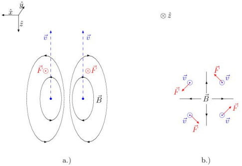

spin sum rule

$$\frac{1}{2} = \frac{1}{2}\Delta\Sigma + \Delta G + \mathcal{L}$$

Longitudinally polarized DIS:

- $\Delta\Sigma = \sum_q \Delta q \equiv \sum_q \int_0^1 dx\,[q_\uparrow(x) - q_\downarrow(x)] \approx 30\%$

$\hookrightarrow$ only small fraction of proton spin due to quark spins

Gluon spin ΔG

could possibly account for remainder of nucleon spin, but still large uncertainties $\rightarrow$ EIC

Quark Orbital Angular Momentum

- how can we measure $\mathcal{L}_{q,g}$

$\hookrightarrow$ need correlation between position & momentum

- how exactly is $\mathcal{L}_{q,g}$ defined

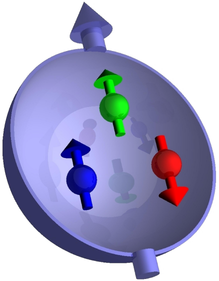

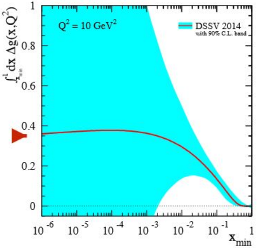

Nucleon Spin Puzzle

spin sum rule

$$\frac{1}{2} = \frac{1}{2}\Delta\Sigma + \Delta G + \mathcal{L}$$

Longitudinally polarized DIS:

- $\Delta\Sigma = \sum_q \Delta q \equiv \sum_q \int_0^1 dx\, [q_\uparrow(x) - q_\downarrow(x)] \approx 30\%$

$\hookrightarrow$ only small fraction of proton spin due to quark spins

Gluon spin ΔG

could possibly account for remainder of nucleon spin, but still large uncertainties $\rightarrow$ EIC

Quark Orbital Angular Momentum

- how can we measure $\mathcal{L}_{q,g}$

$\hookrightarrow$ need correlation between position & momentum

- how exactly is $\mathcal{L}_{q,g}$ defined

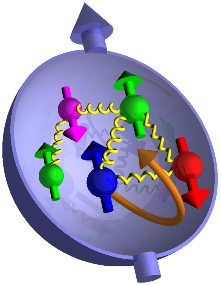

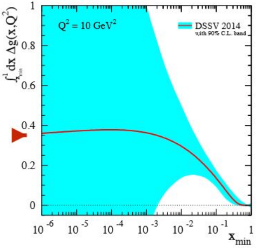

form factor

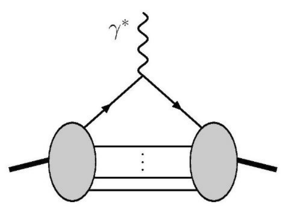

- electron hits nucleon & nucleon remains intact

$\hookrightarrow$ form factor $F(q^2)$

- position information from Fourier trafo
- no sensitivity to quark momentum
- $F(q^2) = \int dx GPD(x, q^2)$

$\hookrightarrow$ GPDs provide momentum disected form factors

Compton scattering

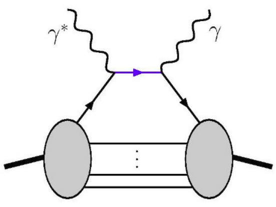

- electron hits nucleon, nucleon remains intact & photon gets emitted
- additional quark propagator

$\hookrightarrow$ additional information about momentum fraction x of active quark

$\hookrightarrow$ generalized parton distributions $GPD(x, q^2)$

- info about both position and momentum of active quark

$q(x, \mathbf{b}_\perp)$ for unpol. p

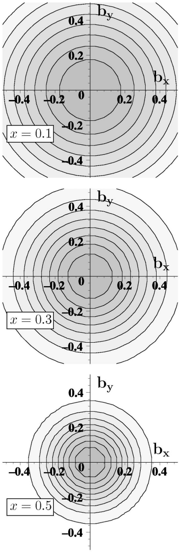

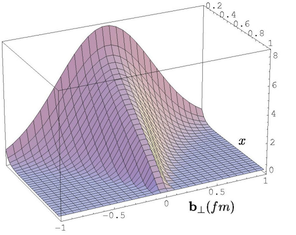

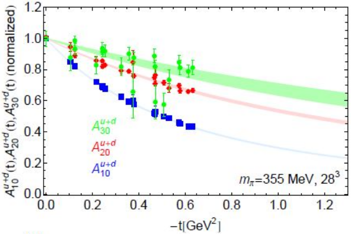

unpolarized proton

- $q(x, \mathbf{b}_\perp) = \int \frac{d^2\Delta_\perp}{(2\pi)^2} H(x, 0, -\mathbf{\Delta}_\perp^2) e^{-i\mathbf{b}_\perp \cdot \mathbf{\Delta}_\perp}$

$\hookrightarrow$ probabilistic interpretation

- $F_1(-\mathbf{\Delta}_\perp^2) = \int dx H(x, 0, -\mathbf{\Delta}_\perp^2)$
- x = momentum fraction of the quark
- $\mathbf{b}_\perp$ relative to $\perp$ center of momentum
- small x: large 'meson cloud'
- larger x: compact 'valence core'
- $x \to 1$: active quark = center of momentum

$\hookrightarrow$ $\vec{b}_\perp \to 0$ (narrow distribution) for $x \to 1$

represents the first fruit of more than a decade of effort in this direction.

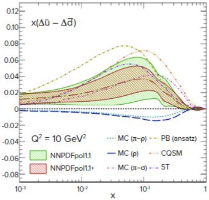

***Figure 2.4:** The difference between the $\Delta\bar{u}$ and $\Delta\bar{d}$ spin functions as extracted from the NNPDF global analysis. The green (red) band shows the present (final expected) uncertainties from analysis of the RHIC W data set. Various model calculations are also shown.*

A Multidimensional View of Nucleon Structure

"With 3D projection, we will be entering a new age. Something which was never technically possible before: a stunning visual experience which 'turbocharges' the viewing." This quotation from film director J. Cameron could just as well describe developments over the last decade or so in hadron physics, in which a multidimensional description of nucleon structure is emerging that is providing profound new insights. Form factors tell us about the distribution of charge and magnetization but contain no direct dynamical information. PDFs allow us to access information on the underlying quarks and their longitudinal momentum but tell us nothing about spatial locations. It has now been established, however, that both form factors and PDFs are special cases of a more general class of distribution functions that merge spatial and dynamic information. Through appropriate measurements, it is becoming possible to construct "pictures" of the nucleon that were never before possible.

3D Spatial Maps of the Nucleon: GPDs

Some of the important new tools for describing hadrons are Generalized Parton Distributions (GPDs). GPDs can be investigated through the analysis of *hard exclusive processes*, processes where the target is probed by high-energy particles and is left intact beyond the production of one or two additional particles. Two processes are recognized as the most powerful processes for accessing GPDs: deeply virtual Compton scattering (DVCS) and deeply virtual meson production (DVMP) where a photon or a meson, respectively, is produced.

One striking way to use GPDs to enhance our understanding of hadronic structure is to use them to construct what we might call 3D spatial maps (see Sidebar 2.2). For a particular value of the momentum fraction *x*, we can construct a spatial map of where the quarks reside. With the JLab 12-GeV Upgrade, the valence quarks will be accurately mapped.

GPDs can also be used to evaluate the total angular momentum associated with different types of quarks, using what is known as the Ji Sum Rule. By combining with other existing data, one can directly access *quark orbital angular momentum*. The worldwide DVCS experimental program, including that at Jefferson Lab with a 6-GeV electron beam and at HERMES with 27-GeV electron and positron beams, has already provided constraints (albeit model dependent) on the total angular momentum of the u and d quarks. These constraints can also be compared with calculations from LQCD. Upcoming 12-GeV experiments at JLab and COMPASS-II experiments at CERN will provide dramatically improved precision. A suite of DVCS and DVMP experiments is planned in Hall B with CLAS12; in Hall A with HRS and existing calorimeters; and in Hall C with HMS, the new SHMS, and the Neutral Particle Spectrometer (NPS). These new data will transform the current picture of hadronic structure.

3D Momentum Maps of the Nucleon: TMDs

Other important new tools for describing nucleon structure are transverse momentum dependent distribution functions (TMDs). These contain information on both the longitudinal and transverse momentum of the quarks (and gluons) inside a fast moving nucleon. TMDs link the transverse motion of the quarks with their spin and/or the spin of the parent proton and are, thus, sensitive to orbital angular momentum. Experimentally, these functions can be investigated in proton-proton collisions, in inclusive production of lepton pairs in Drell-Yan processes, and in *semi-inclusive deep inelastic scattering* (SIDIS), where one measures the scattered electron and one more meson (typically a pion or kaon) in the DIS process.

Sidebar 2.2: The First 3D Pictures of the Nucleon

A computed tomography (CT) scan can help physicians pinpoint minute cancer tumors, diagnose tiny broken bones, and spot the early signs of osteoporosis. Now physicists are using the principles behind the procedure to peer at the inner workings of the proton. This breakthrough is made possible by a relatively new concept in nuclear physics called generalized parton distributions.

An intense beam of high-energy electrons can be used as a microscope to look inside the proton. The high energies tend to disrupt the proton, so one or more new particles are produced. Physicists often disregarded what happened to the debris and measured only the energy and position of the scattered electron. This method is called inclusive deep inelastic scattering and has revealed the most basic grains of matter, the quarks. However, it has a limitation: it can only give a one-dimensional image of the substructure of the proton because it essentially measures the momentum of the quarks along the direction of the incident electron beam. To provide the three-dimensional (3D) picture, we need instead to measure all the particles in the debris. This way, we can construct a 3D image of the proton as successive spatial quark distributions in planes perpendicular to its motion for slices in the quark's momentum, just like a 3D image of the human body can be built from successive planar views.

An electron can scatter from a proton in many ways. We are interested in those collisions where a high-energy electron strikes an individual quark inside the proton, giving the quark a very large amount of extra energy. This quark then quickly gets rid of its excess energy, for instance, by emitting a high-energy photon. The quark does not change identity and remains part of the intact target proton. This specific process is called deeply virtual Compton scattering (DVCS). For the experiment to work, the scientists need to measure the speed, position, and energy of the electron that bounced off the quark, of the photon emitted by the quark, and of the reassembled proton. From this information the 3D picture of the proton can be constructed.

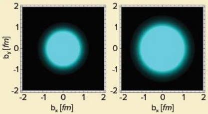

The first 3D views of the proton: the spatial charge densities of the proton in a plane (bx, by) positioned at two different values of the quark's longitudinal momentum x: 0.25 (left) and 0.09 (right).

Very recently, using the DVCS data collected with the CLAS detector at JLab and the HERMES detector at DESY/Germany, the first nearly model-independent images of the proton started to appear. The result of this work is illustrated in the figure, where the probabilities for the quarks to reside at various places inside the proton are shown at two different values of its longitudinal momentum x (x = 0.25 left and x = 0.09 right). This is analogous to the "orbital" clouds used to depict the likely position of electrons in various energy levels inside atoms. The first 3D pictures of the proton indicate that when the longitudinal momentum x of the quark decreases, the radius of the proton increases.

The broader implications of these results are that we now have methods to fill in the information needed to extract 3D views of the proton. Physicists worldwide are working toward this goal, and the technique pioneered here will be applied with Jefferson Lab's CEBAF accelerator at 12 GeV for (valence) quarks and, later, with a future EIC for gluons and sea quarks.

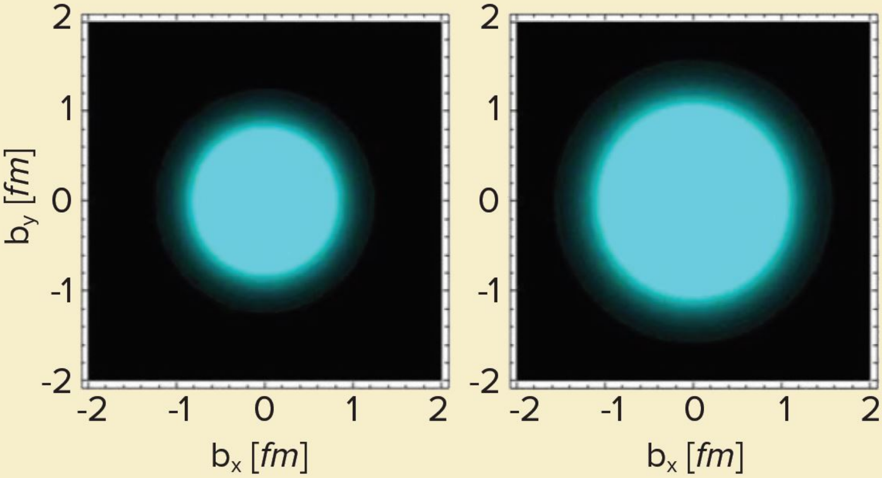

The first 3D views of the proton: the spatial charge densities of the proton in a plane (bx, by) positioned at two different values of the quark's longitudinal momentum x: 0.25 (left) and 0.09 (right).

$\perp$ imaging: $\xi \neq 0$

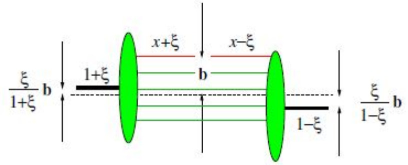

- center of momentum of hadron not 'conserved' when $\xi \neq 0$,

$\hookrightarrow$ distance of active quark to COM not conserved

- $\perp$ position of each parton is conserved, and so is (any ξ)

$\hookrightarrow$ distance $\mathbf{r}_\perp$ of active quark to spectators (any ξ)

- variable conjugate to $\Delta_\perp$ is $\frac{1-x}{1-\xi}\mathbf{r}_\perp$

$\perp$ imaging: $\xi = 0$

- probabilistic interpretation
- variable conjugate to $\Delta_\perp$ is $\mathbf{b}_\perp \equiv (1-x)\mathbf{r}_\perp$ distance to COM of hadron

$\perp$ imaging $(x = \xi)$

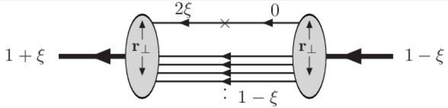

- no probabilistic interpretation
- still meaningful to think about 'size' of overlap matrix element
- variable conjugate to $\mathbf{\Delta}_\perp$ is $\mathbf{r}_\perp$ distance to COM of spectators
- $t = t_0 - \frac{1+\xi}{1-\xi}\Delta_\perp^2$

$\hookrightarrow$ t-slope $\neq$ $\Delta_\perp^2$-slope

Physics of GPDs: 3D Imaging MB, IJMPA 18, 173 (2003)

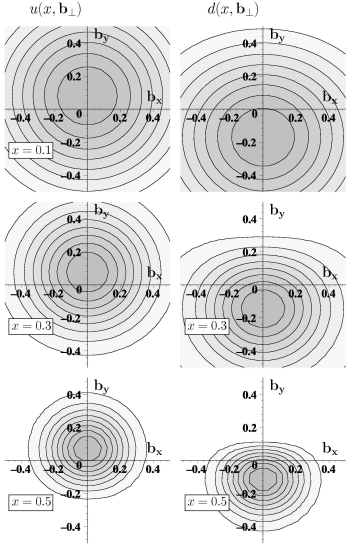

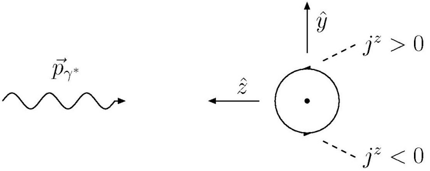

proton polarized in $+\hat{x}$ direction

$$q(x, \mathbf{b}_\perp) = \int \frac{d^2\Delta_\perp}{(2\pi)^2} H_q(x,0,-\Delta_\perp^2) e^{-i\mathbf{b}_\perp\cdot\Delta_\perp}$$
$$-\frac{1}{2M}\frac{\partial}{\partial b_y}\int \frac{d^2\Delta_\perp}{(2\pi)^2} E_q(x,0,-\Delta_\perp^2) e^{-i\mathbf{b}_\perp\cdot\Delta_\perp}$$

- relevant density in DIS is $j^+ \equiv j^0 + j^z$ and left-right asymmetry from j^z
- av. shift model-independently related to anomalous magnetic moments:

$$\langle b_y^q \rangle \equiv \int dx \int d^2 b_\perp q(x, \mathbf{b}_\perp) b_y = \frac{1}{2M}\int dx E_q(x,0,0) = \frac{\kappa_q}{2M}$$

example: $\gamma p \rightarrow \pi X$

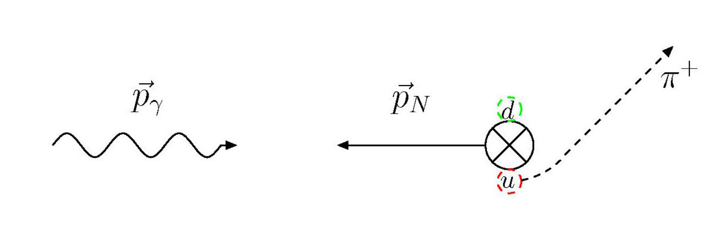

- u, d distributions in $\perp$ polarized proton have left-right asymmetry in $\perp$ position space (T-even!); sign "determined" by κ_u & κ_d
- attractive final state interaction (FSI) deflects active quark towards the center of momentum

$\hookrightarrow$ FSI translates position space distortion (before the quark is knocked out) in $+\hat{y}$-direction into momentum asymmetry that favors $-\hat{y}$ direction $\rightarrow$ chromodynamic lensing

$\Rightarrow$ $\kappa_p\,,\kappa_n \quad \longleftrightarrow \quad$ sign of SSA!!!!!!!! (MB,2004)

- confirmed by HERMES & COMPASS data

- $L_x = yp_z - zp_y$
- if state invariant under rotations about $\hat{x}$ axis then $\langle yp_z \rangle = -\langle zp_y \rangle$

$\hookrightarrow$ $\langle L_x \rangle = 2\langle yp_z \rangle$

- GPDs provide simultaneous information about longitudinal momentum and transverse position

$\hookrightarrow$ use quark GPDs to determine angular momentum carried by quarks

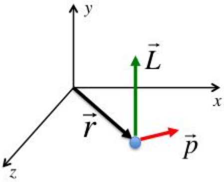

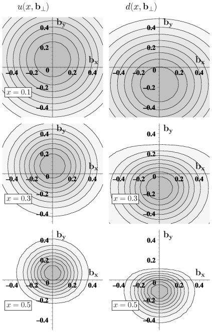

Ji sum rule (1996)

$$J_q^x = \frac{1}{2}\int dx\, x\,[H(x,0,0) + E(x,0,0)]$$

- parton interpretation in terms of 3D distributions only for $\perp$ component (MB,2001,2005)

lattice: (lattice hadron physics collaboration - LHPC)

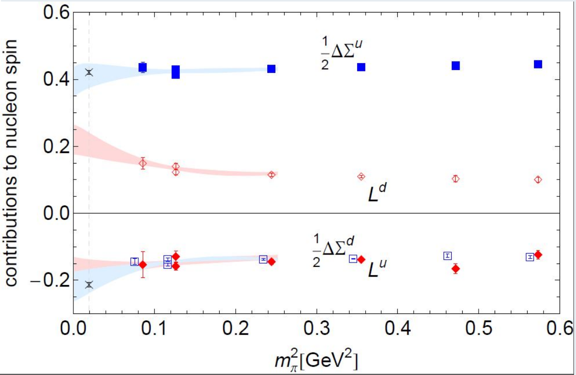

- no disconnected quark loops
- chiral extrapolation

$$J^q = \frac{1}{2}\int dx\, x\,[H(x,0,0) + E(x,0,0)] \qquad L^q = J^q - \frac{1}{2}\Delta\Sigma^q$$

QED with electrons

$$\vec{J}_\gamma = \int d^3r\,\vec{r}\times\left(\vec{E}\times\vec{B}\right) = \int d^3r\,\vec{r}\times\left[\vec{E}\times\left(\vec{\nabla}\times\vec{A}\right)\right]$$
$$= \int d^3r\,\left[E^j\left(\vec{r}\times\vec{\nabla}\right)A^j - \vec{r}\times(\vec{E}\cdot\vec{\nabla})\vec{A}\right]$$
$$= \int d^3r\,\left[E^j\left(\vec{r}\times\vec{\nabla}\right)A^j + \left(\vec{r}\times\vec{A}\right)\vec{\nabla}\cdot\vec{E} + \vec{E}\times\vec{A}\right]$$

- replace 2^{nd} term (eq. of motion $\vec{\nabla}\cdot\vec{E} = ej^0 = e\psi^\dagger\psi$), yielding

$$\vec{J}_\gamma = \int d^3r\left[\psi^\dagger\vec{r}\times e\vec{A}\psi + E^j\left(\vec{x}\times\vec{\nabla}\right)A^j + \vec{E}\times\vec{A}\right]$$

- $\psi^\dagger\vec{r}\times e\vec{A}\psi$ cancels similar term in electron OAM $\psi^\dagger\vec{r}\times(\vec{p}-e\vec{A})\psi$

$\hookrightarrow$ decomposing $\vec{J}_\gamma$ into spin and orbital also shuffles angular momentum from photons to electrons!

The Nucleon Spin Pizzas

Ji decomposition

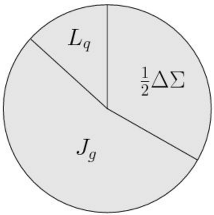

'pizza tre stagioni'

$$\frac{1}{2} = \sum_q \left(\frac{1}{2}\Delta q + L_q\right) + J_g$$

$$\frac{1}{2}\Delta q = \frac{1}{2}\int d^3x \, \langle P,S|\, q^\dagger(\vec{x})\Sigma^3 q(\vec{x})\,|P,S\rangle$$

$$L_q = \int d^3x \langle P,S| q^\dagger(\vec{x})\left(\vec{x}\times i\vec{D}\right)^3 q(\vec{x})|P,S\rangle$$

$$J_g = \int d^3x \, \langle P,S|\left[\vec{x}\times\left(\vec{E}\times\vec{B}\right)\right]^z |P,S\rangle$$

- $i\vec{D} = i\vec{\partial} - g\vec{A}$

Jaffe-Manohar decomposition

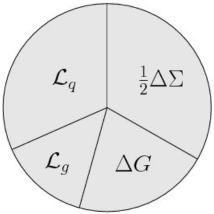

'pizza quattro stagioni'

$$\frac{1}{2} = \sum_q \left(\frac{1}{2}\Delta q + \mathcal{L}_q\right) + \Delta G + \mathcal{L}_g$$

light-cone gauge $A^+ = 0$

$$\mathcal{L}_q = \int d^3r \langle P,S|\, \bar{q}(\vec{r})\gamma^+\left(\vec{r}\times i\vec{\partial}\right)^z q(\vec{r})|P,S\rangle$$

$$\Delta G = \varepsilon^{+-ij}\int d^3r \, \langle P,S|\, \mathrm{Tr} F^{+i} A^j \,|P,S\rangle$$

$$\mathcal{L}_g = 2\int d^3r \langle P,S| \mathrm{Tr} F^{+j}\left(\vec{x}\times i\vec{\partial}\right)^z A^j |P,S\rangle$$

manifestly gauge inv. def. for each term exists (Lorcé, Pasquini; Hatta)

The Nucleon Spin Pizzas

Ji decomposition

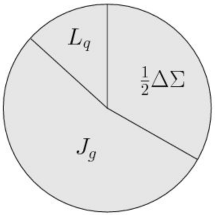

'pizza tre stagioni'

$$\frac{1}{2} = \sum_q \left(\frac{1}{2}\Delta q + L_q\right) + J_g$$

$$L_q = \int d^3x \langle P,S| q^\dagger(\vec{x}) \left(\vec{x} \times i\vec{D}\right)^3 q(\vec{x}) |P,S\rangle$$

- $i\vec{D} = i\vec{\partial} - g\vec{A}$
- DVCS $\longrightarrow$ GPDs $\longrightarrow L^q$

Jaffe-Manohar decomposition

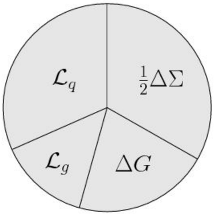

'pizza quattro stagioni'

$$\frac{1}{2} = \sum_q \left(\frac{1}{2}\Delta q + \mathcal{L}_q\right) + \Delta G + \mathcal{L}_g$$

$$\mathcal{L}_q = \int d^3r \langle P,S| \bar{q}(\vec{r})\gamma^+ \left(\vec{r} \times i\vec{\partial}\right)^z q(\vec{r}) |P,S\rangle$$

- light-cone gauge $A^+ = 0$
- $\vec{p}\,\overleftarrow{p} \longrightarrow \Delta G \longrightarrow \mathcal{L} \equiv \sum_{i\in q,g} \mathcal{L}^i$

How large is difference $\mathcal{L}_q - L_q$ in QCD and what does it represent?

5-D Wigner Functions (Lorcé, Pasquini)

$$W(x,\vec{b}_\perp,\vec{k}_\perp) \equiv \int \frac{d^2\vec{q}_\perp}{(2\pi)^2}\int \frac{d^2\xi_\perp d\xi^-}{(2\pi)^3} e^{ik\cdot\xi} e^{-i\vec{q}_\perp\cdot\vec{b}_\perp} \langle P'S'|\bar{q}(0)\gamma^+ q(\xi)|PS\rangle.$$

- TMDs: $f(x,\mathbf{k}_\perp) = \int d^2\mathbf{b}_\perp W(x,\vec{b}_\perp,\vec{k}_\perp)$
- GPDs: $q(x,\mathbf{b}_\perp) = \int d^2\mathbf{k}_\perp W(x,\vec{b}_\perp,\vec{k}_\perp)$
- $L_z = \int dx \int d^2\mathbf{b}_\perp \int d^2\mathbf{k}_\perp W(x,\vec{b}_\perp,\vec{k}_\perp)(b_x k_y - b_y k_x)$
- need to include Wilson-line gauge link $\mathcal{U}_{0\xi} \sim \exp\left(i\frac{g}{\hbar}\int_0^\xi \vec{A}\cdot d\vec{r}\right)$ to connect 0 and ξ

$\hookrightarrow$ crucial for SSAs in SIDIS et al.

straight line for $\mathcal{U}_{0\xi}$

straigth Wilson line from 0 to ξ yields Ji-OAM:

$$L^q = \int d^3x \langle P,S|q^\dagger(\vec{x})\left(\vec{x}\times i\vec{D}\right)^z q(\vec{x})|P,S\rangle$$

Light-Cone Staple for $\mathcal{U}_{0\xi}$

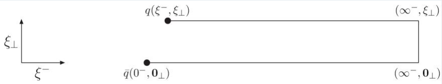

'light-cone staple' yields $\mathcal{L}_{Jaffe-Manohar}$

$\mathcal{L}_{\sqsupset}/\mathcal{L}_{\sqsubset}$

$\mathcal{L}$ with light-cone staple at $x^- = \pm\infty$

PT (Hatta)

- PT$\longrightarrow$ $\mathcal{L}_{\sqsupset} = \mathcal{L}_{\sqsubset}$

(different from SSAs due to factor $\vec{x}$ in OAM)

Bashinsky-Jaffe

- $A^+ = 0$ no complete gauge fixing

$\hookrightarrow$ residual gauge inv. $A^\mu \rightarrow A^\mu + \partial^\mu \phi(\vec{x}_\perp)$

- $\vec{x} \times i\vec{\partial} \quad \rightarrow \quad \mathcal{L}_{JB} \equiv \vec{x} \times \left[i\vec{\partial} - g\vec{\mathcal{A}}(\vec{x}_\perp) \right]$
- $\vec{\mathcal{A}}_\perp(\vec{x}_\perp) = \frac{\int dx^- \vec{A}_\perp(x^-, \vec{x}_\perp)}{\int dx^-}$

Bashinsky-Jaffe $\leftrightarrow$ light-cone staple

- $A^+ = 0$

$\hookrightarrow$ $\mathcal{L}_{\sqsupset/\sqsubset} = \vec{x} \times \left[i\vec{\partial} - g\vec{A}_\perp(\pm\infty, \vec{x}_\perp) \right]$

- $\mathcal{L}_{JB} = \vec{x} \times \left[i\vec{\partial} - g\vec{\mathcal{A}}(\vec{x}_\perp) \right]$
- $\vec{\mathcal{A}}_\perp(\vec{x}_\perp) = \frac{\int dx^- \vec{A}_\perp(x^-, \vec{x}_\perp)}{\int dx^-} = \frac{1}{2}\left(\vec{A}_\perp(\infty, \vec{x}_\perp) + \vec{A}_\perp(-\infty, \vec{x}_\perp) \right)$

$\hookrightarrow$ $\mathcal{L}_{JB} = \frac{1}{2}\left(\mathcal{L}_{\sqsupset} + \mathcal{L}_{\sqsubset} \right) = \mathcal{L}_{\sqsupset} = \mathcal{L}_{\sqsubset}$

straight line ($\rightarrow$Ji)

$$\frac{1}{2} = \sum_q \frac{1}{2}\Delta q + L_q + J_g$$

$$L_q = \int d^3x \langle P,S|\bar{q}(\vec{x})\gamma^+\left(\vec{x}\times i\vec{D}\right)^z q(\vec{x})|P,S\rangle$$

- $i\vec{D} = i\vec{\partial} - g\vec{A}$

light-cone staple ($\rightarrow$ Jaffe-Manohar)

$$\frac{1}{2} = \sum_q \frac{1}{2}\Delta q + \mathcal{L}_q + \Delta G + \mathcal{L}_g$$

$$\mathcal{L}^q = \int d^3x \langle P,S|\bar{q}(\vec{x})\gamma^+\left(\vec{x}\times i\vec{\mathcal{D}}\right)^z q(\vec{x})|P,S\rangle$$

$$i\vec{\mathcal{D}} = i\vec{\partial} - g\vec{A}(x^- = \infty, \mathbf{x}_\perp)$$

difference $\mathcal{L}^q - L^q$

$$\mathcal{L}^q - L^q = -g\int d^3x \langle P,S|\bar{q}(\vec{x})\gamma^+\left[\vec{x}\times \int_{x^-}^{\infty} dr^- F^{+\perp}(r^-,\mathbf{x}_\perp)\right]^z q(\vec{x})|P,S\rangle$$

$$\sqrt{2}F^{+y} = F^{0y} + F^{zy} = -E^y + B^x$$

straight line ($\to$Ji)

$$\frac{1}{2} = \sum_q \frac{1}{2}\Delta q + L_q + J_g$$

$$L_q = \int d^3x \langle P,S|\bar{q}(\vec{x})\gamma^+\left(\vec{x} \times i\vec{D}\right)^z q(\vec{x})|P,S\rangle$$

- $i\vec{D} = i\vec{\partial} - g\vec{A}$

light-cone staple ($\to$ Jaffe-Manohar)

$$\frac{1}{2} = \sum_q \frac{1}{2}\Delta q + \mathcal{L}_q + \Delta G + \mathcal{L}_g$$

$$\mathcal{L}^q = \int d^3x \langle P,S|\bar{q}(\vec{x})\gamma^+\left(\vec{x} \times i\vec{\mathcal{D}}\right)^z q(\vec{x})|P,S\rangle$$

$$i\mathcal{D}^j = i\partial^j - gA^j(x^-, \mathbf{x}_\perp) - g\int_{x^-}^\infty dr^- F^{+j}$$

difference $\mathcal{L}^q - L^q$

$$\mathcal{L}^q - L^q = -g\int d^3x \langle P,S|\bar{q}(\vec{x})\gamma^+\left[\vec{x} \times \int_{x^-}^\infty dr^- F^{+\perp}(r^-, \mathbf{x}_\perp)\right]^z q(\vec{x})|P,S\rangle$$

color Lorentz Force on ejected quark (MB, PRD 88 (2013) 014014)

$$\sqrt{2}F^{+y} = F^{0y} + F^{zy} = -E^y + B^x = -\left(\vec{E} + \vec{v} \times \vec{B}\right)^y \text{ for } \vec{v} = (0,0,-1)$$

straight line ($\rightarrow$Ji)

$$\frac{1}{2} = \sum_q \frac{1}{2}\Delta q + L_q + J_g$$

$$L_q = \int d^3x \langle P,S|\bar{q}(\vec{x})\gamma^+\left(\vec{x}\times i\vec{D}\right)^z q(\vec{x})|P,S\rangle$$

- $i\vec{D} = i\vec{\partial} - g\vec{A}$

light-cone staple ($\rightarrow$ Jaffe-Manohar)

$$\frac{1}{2} = \sum_q \frac{1}{2}\Delta q + \mathcal{L}_q + \Delta G + \mathcal{L}_g$$

$$\mathcal{L}^q = \int d^3x \langle P,S|\bar{q}(\vec{x})\gamma^+\left(\vec{x}\times i\vec{\mathcal{D}}\right)^z q(\vec{x})|P,S\rangle$$

$$i\mathcal{D}^j = i\partial^j - gA^j(x^-,\mathbf{x}_\perp) - g\int_{x^-}^\infty dr^- F^{+j}$$

difference $\mathcal{L}^q - L^q$

$$\mathcal{L}^q - L^q = -g\int d^3x \langle P,S|\bar{q}(\vec{x})\gamma^+\left[\vec{x}\times \int_{x^-}^\infty dr^- F^{+\perp}(r^-,\mathbf{x}_\perp)\right]^z q(\vec{x})|P,S\rangle$$

color Lorentz Force on ejected quark (MB, PRD 88 (2013) 014014)

$$\sqrt{2}F^{+y} = F^{0y} + F^{zy} = -E^y + B^x = -\left(\vec{E} + \vec{v}\times\vec{B}\right)^y \text{ for } \vec{v} = (0,0,-1)$$

Torque along the trajectory of q

$$T^z = \left[\vec{x}\times\left(\vec{E} - \hat{\vec{z}}\times\vec{B}\right)\right]^z$$

Change in OAM

$$\Delta L^z = \int_{x^-}^\infty dr^- \left[\vec{x}\times\left(\vec{E} - \hat{\vec{z}}\times\vec{B}\right)\right]^z$$

(Ji et al., 2016)

- for e^-: $\mathcal{L}_{JM} - L_{Ji} = 0$ to $\mathcal{O}(\alpha)$
- $\mathcal{L}_{JM} - L_{Ji} \stackrel{?}{=} 0$ in general?
- how significant is $\mathcal{L}_{JM} - L_{Ji}$?

why scalar diquark model?

- Lorentz invariant
- 1^{st} to illustrate: FSI→SSAs (Brodsky,Hwang,Schmidt 2002)

$\hookrightarrow$ Sivers $\neq 0$

$\mathcal{L}_{JM} - L_{Ji} = \langle \bar{q}\gamma^+ \left(\vec{r} \times \vec{A}\right)^z q\rangle$ in scalar diquark model

- pert. evaluation of $\langle \bar{q}\gamma^+ \left(\vec{r} \times \vec{A}\right)^z q\rangle$

$\hookrightarrow$ $\mathcal{L}_{JM} - L_{Ji} = \mathcal{O}(\alpha)$

- same order as Sivers

$\hookrightarrow$ $\mathcal{L}_{JM} - L_{Ji}$ as significant as SSAs

calculation

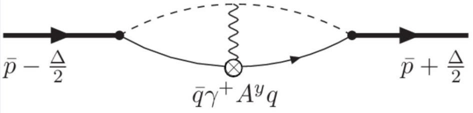

- nonforward matrix elem. of $\bar{q}\gamma^+ A^y q$
- $\left.\frac{d}{d\Delta^x}\right|_{\Delta=0}$

$\hookrightarrow$ $\langle k_\perp^q \rangle = \frac{3m_q+M}{12}\pi \langle \bar{q}\gamma^+ \left(\vec{r} \times \vec{A}\right)^z q\rangle$

difference $\mathcal{L}^q - L^q$

$\mathcal{L}^q_{JM} - L^q_{Ji} = \Delta L^q_{FSI}$ = change in OAM as quark leaves nucleon

$$\mathcal{L}^q_{JM} - L^q_{Ji} = -g \int d^3x \langle P,S|\bar{q}(\vec{x})\gamma^+\left[\vec{x}\times\int_{x^-}^{\infty} dr^- F^{+\perp}(r^-,\mathbf{x}_\perp)\right]^z q(\vec{x})|P,S\rangle$$

e^+ moving through dipole field of e^-

- consider e^- polarized in $+\hat{z}$ direction

$\hookrightarrow$ $\vec{\mu}$ in $-\hat{z}$ direction (Figure)

- e^+ moves in $-\hat{z}$ direction

$\hookrightarrow$ net torque negative

sign of $\mathcal{L}^q - L^q$ in QCD

- color electric force between two q in nucleon attractive

$\hookrightarrow$ same as in positronium

- spectator spins positively correlated with nucleon spin

$\hookrightarrow$ expect $\mathcal{L}^q - L^q < 0$ in nucleon

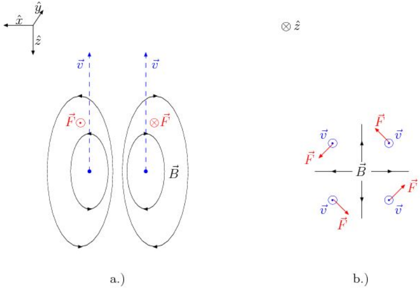

difference $\mathcal{L}^q - L^q$

$\mathcal{L}^q_{JM} - L^q_{Ji} = \Delta L^q_{FSI}$ = change in OAM as quark leaves nucleon

$$\mathcal{L}^q_{JM} - L^q_{Ji} = -g \int d^3x \langle P,S|\bar{q}(\vec{x})\gamma^+\left[\vec{x}\times \int_{x^-}^{\infty} dr^- F^{+\perp}(r^-,\mathbf{x}_\perp)\right]^z q(\vec{x})|P,S\rangle$$

e^+ moving through dipole field of e^-

- consider e^- polarized in $+\hat{z}$ direction
- $\hookrightarrow$ $\vec{\mu}$ in $-\hat{z}$ direction (Figure)
- e^+ moves in $-\hat{z}$ direction
- $\hookrightarrow$ net torque negative

sign of $\mathcal{L}^q - L^q$ in QCD

- color electric force between two q in nucleon attractive
- $\hookrightarrow$ same as in positronium
- spectator spins positively correlated with nucleon spin
- $\hookrightarrow$ expect $\mathcal{L}^q - L^q < 0$ in nucleon

lattice QCD (M.Engelhardt)

- L_{staple} vs. staple length
- $\hookrightarrow$ L^q_{Ji} for length $= 0$
- $\hookrightarrow$ $\mathcal{L}^q_{JM}$ for length $\to \infty$

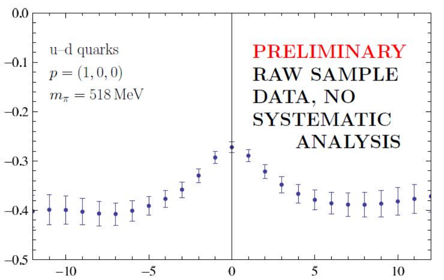

- shown $L^u_{staple} - L^d_{staple}$
- similar result for each ΔL^q_{FSI}

difference $\mathcal{L}^q - L^q$

$$\mathcal{L}^q_{JM} - L^q_{Ji} = -g \int d^3x \langle P,S|\bar{q}(\vec{x})\gamma^+\left[\vec{x}\times\int_{x^-}^{\infty} dr^- F^{+\perp}(r^-,\mathbf{x}_\perp)\right]^z q(\vec{x})|P,S\rangle$$

- change in OAM as quark leaves nucleon due to torque from FSI on active quark

color Lorentz Force on ejected quark (MB, PRD 88 (2013) 014014)

$$\sqrt{2}F^{+y} = F^{0y} + F^{zy} = -E^y + B^x = -\left(\vec{E} + \vec{v}\times\vec{B}\right)^y \text{ for } \vec{v} = (0,0,-1)$$

Single-Spin Asymmetries (Qiu-Sterman)

- $\perp$ single-spin asymmetry in semi-inclusive DIS governed by 'Qiu-Sterman integral'

$$\langle P,S|\bar{q}(\vec{x})\gamma^+\int_{x^-}^{\infty} dr^- F^{+\perp}(r^-,\mathbf{x}_\perp) q(\vec{x})|P,S\rangle = 0$$

- semi-classical interpretation: $F^{+\perp}(r^-,\mathbf{x}_\perp)$ color Lorentz Force acting on active quark on its way out

$\hookrightarrow$ integral yields $\perp$ impulse due to FSI

$\mathcal{A}_{DVCS} \overset{?}{\rightsquigarrow} GPDs$

interesting GPD physics:

- $J_q = \int_0^1 dx x\,[H(x,\xi,0) + E(x,\xi,0)]$ requires $GPDs(x,\xi,0)$ for (common) fixed ξ for all x
- $\perp$ imaging requires $GPDs(x, \xi = 0, t)$

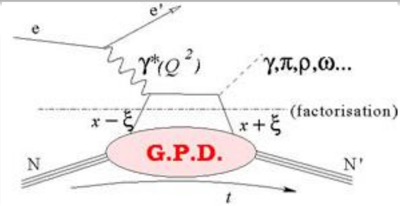

- ξ longitudinal momentum transfer on the target $\xi = \frac{p^{+\prime} - p^{+}}{p^{+\prime} + p^{+}}$
- x (average) momentum fraction of the active quark $x = \frac{k^{+\prime} + p^{+}}{p^{+\prime} + p^{+}}$

$\Im \mathcal{A}_{DVCS}(\xi, t) \longrightarrow GPD(\xi, \xi, t)$

- only sensitive to 'diagonal' $x = \xi$
- limited ξ range

$\Re \mathcal{A}_{DVCS}(\xi, t) \longrightarrow \int_{-1}^{1} dx \frac{GPD(x,\xi,t)}{x-\xi}$

- limited ξ range
- most sensitive to $x \approx \xi$
- some sensitivity to $x \neq \xi$, but

Polynomiality/Dispersion Relations (GPV/AT DI)

$$\Re \mathcal{A}(\xi, t, Q^2) = \int_{-1}^{1} dx \frac{H(x, \xi, t, Q^2)}{x - \xi} = \int_{-1}^{1} dx \frac{H(x, x, t, Q^2)}{x - \xi} + \Delta(t, Q^2)$$

$\mathcal{A}_{DVCS} \overset{?}{\rightsquigarrow} GPDs$

interesting GPD physics:

- $J_q = \int_0^1 dx x \, [H(x,\xi,0) + E(x,\xi,0)]$ requires $GPDs(x,\xi,0)$ for (common) fixed ξ for all x
- $\perp$ imaging requires $GPDs(x, \xi = 0, t)$

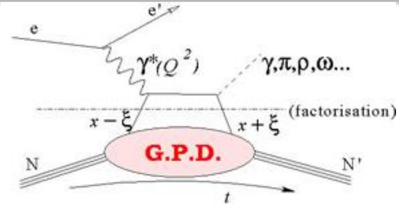

$\Im\mathcal{A}_{DVCS}(\xi,t) \longrightarrow GPD(\xi,\xi,t)$

$\Re\mathcal{A}_{DVCS}(\xi,t) \longrightarrow \int_{-1}^{1} dx \frac{GPD(x,\xi,t)}{x-\xi}$

Polynomiality/Dispersion Relations (GPV/AT DI)

$$\Re\mathcal{A}(\xi,t,Q^2) = \int_{-1}^{1} dx \frac{H(x,\xi,t,Q^2)}{x-\xi} = \int_{-1}^{1} dx \frac{H(x,x,t,Q^2)}{x-\xi} + \Delta(t,Q^2)$$

- Can 'condense' all information contained in contained in $\mathcal{A}_{DVCS}$ (fixed Q^2) into $GPD(x,x,t,Q^2)$ & $\Delta(t,Q^2)$
- if two models both satisfy polynomiality and are equal for $x = \xi$ (but not for $x \neq \xi$) and have same $\Delta(t,Q^2)$ then DVCS at fixed Q^2 cannot distinguish between the two models

$\mathcal{A}_{DVCS} \overset{?}{\rightsquigarrow} GPDs$

Polynomiality/Dispersion Relations (GPV/AT DI)

$$\Re\mathcal{A}(\xi,t,Q^2) = \int_{-1}^{1} dx \frac{H(x,\xi,t,Q^2)}{x-\xi} = \int_{-1}^{1} dx \frac{H(x,x,t,Q^2)}{x-\xi} + \Delta(t,Q^2)$$

- Can 'condense' all information contained in $\mathcal{A}_{DVCS}$ (fixed Q^2) into $GPD(x,x,t,Q^2)$ & $\Delta(t,Q^2)$
- if two models both satisfy polynomiality and are equal for $x = \xi$ (but not for $x \neq \xi$) and have same $\Delta(t,Q^2)$ then DVCS at fixed Q^2 cannot distinguish between the two models

need Evolution! → JLab, Compass, EIC

$$\mu^2 \frac{d}{d\mu^2} H^{q(-)}(x,\xi,t) = \int_{-1}^{1} dx' \frac{1}{|\xi|} V_{\mathrm{NS}}\left(\frac{x}{\xi},\frac{x'}{\xi}\right) H^{q(-)}(x',\xi,t)$$

- Q^2 evolution changes x distribution in a known way for fixed ξ

↪ measure Q^2 dependence to disentangle x vs. ξ dependence

- GPDs $\xrightarrow{FT}$ $q(x, \mathbf{b}_\perp)$ '3d imaging'
- $\perp$ polarization $\Rightarrow \perp$ deformation
- simultaneous info about $\perp$ position & long. momentum

$\hookrightarrow$ Ji sum rule for J_q

- $\mathcal{L}^q_{JM} - L^q_{Ji}$ = change in OAM as quark leaves nucleon (due to torque from FSI)

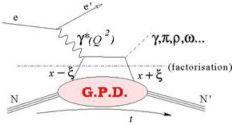

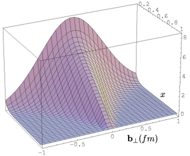

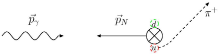

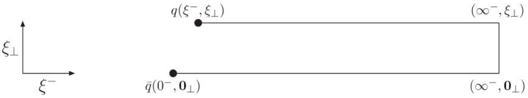

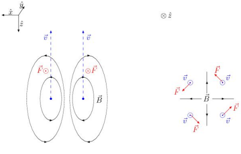

a.) b.)

challenge

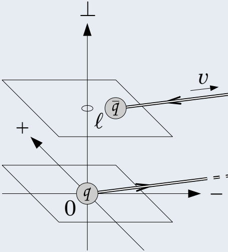

- TMDs/Wigner functions relevant for SIDIS require (near) light-like Wilson lines
- on Euclidean lattice, all distances are space-like

TMDs in lattice QCD

B. Musch, P. Hägler, M. Engelhardt

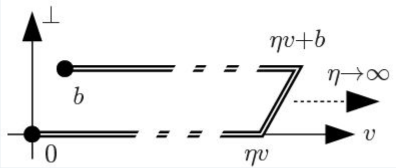

- calculate space-like staple-shaped Wilson line pointing in $\hat{z}$ direction; length $L \to \infty$
- momentum projected nucleon sources/sinks
- remove IR divergences by considering appropriate ratios

$\hookrightarrow$ extrapolate/evolve to $P_z \to \infty$

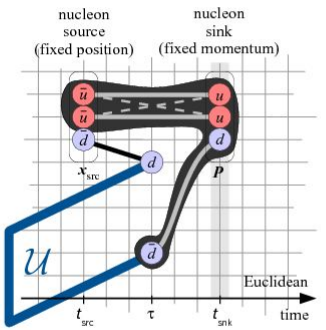

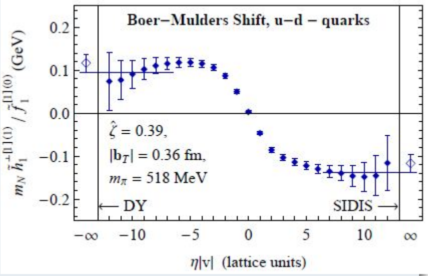

$f_{1T,SIDIS}^{\perp} = -f_{1T,DY}^{\perp}$ (Collins)

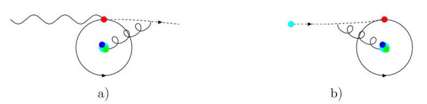

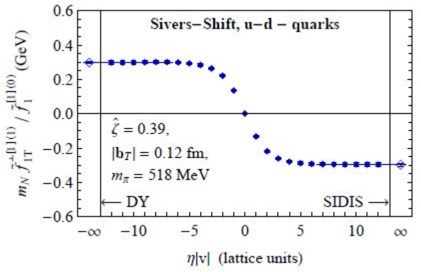

$f_{1T}^{\perp}(x, \mathbf{k}_\perp)$ is $\mathbf{k}_\perp$-odd term in quark-spin averaged momentum distribution in $\perp$ polarized target

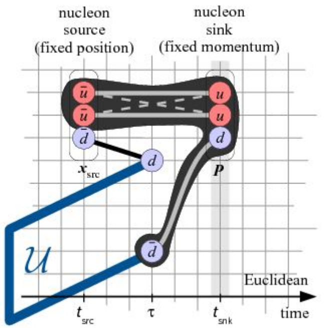

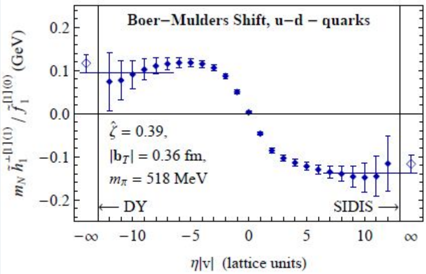

$f_{1T,SIDIS}^{\perp} = -f_{1T,DY}^{\perp}$ (Collins)

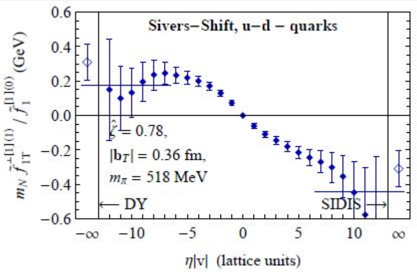

$f_{1T}^{\perp}(x, \mathbf{k}_\perp)$ is $\mathbf{k}_\perp$-odd term in quark-spin averaged momentum distribution in $\perp$ polarized target